

Topology-preserving Adversarial Training for Alleviating Natural Accuracy Degradation

Xiaoyue Mi^{1,2}

mixiaoyue19s@ict.ac.cn

Fan Tang^{*1,2}

fan.108@gmail.com

Yepeng Weng^{1,2}

wengyepeng15@mails.ucas.ac.cn

Danding Wang^{1,2}

wangdanding@ict.ac.cn

Juan Cao^{1,2}

caojuan@ict.ac.cn

Sheng Tang^{1,2}

st@ict.ac.cn

Peng Li^{*3}

mpeng@air.tsinghua.edu.cn

Yang Liu^{3,4}

liuyang2011@tsinghua.edu.cn

¹ Institute of Computing Technology, Chinese Academy of Sciences (CAS), Beijing, China

² University of Chinese Academy of Sciences, Beijing, China

³ Institute for AI Industry Research (AIR), Tsinghua University, Beijing, China

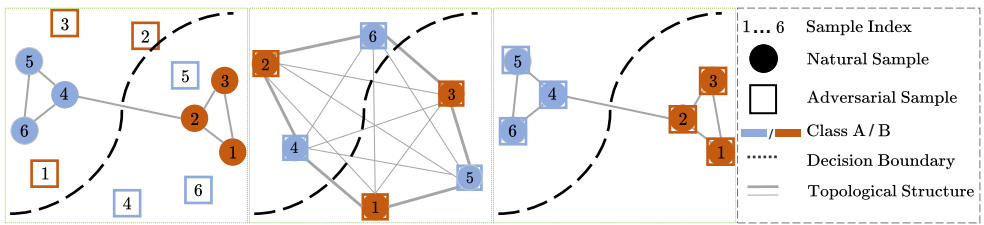
⁴ Department of Computer Science & Technology, Tsinghua University, Beijing, China

Abstract

Despite the effectiveness in improving the robustness of neural networks, adversarial training has suffered from the natural accuracy degradation problem, i.e., accuracy on natural samples has reduced significantly. In this study, we reveal that natural accuracy degradation is highly related to the disruption of the natural sample topology in the representation space by quantitative and qualitative experiments. Based on this observation, we propose Topology-pReserving Adversarial traINing (TRAIN) to alleviate the problem by preserving the topology structure of natural samples from a standard model trained only on natural samples during adversarial training. As an additional regularization, our method can be combined with various popular adversarial training algorithms, taking advantage of both sides. Extensive experiments on CIFAR-10, CIFAR-100, and Tiny ImageNet show that our proposed method achieves consistent and significant improvements over various strong baselines in most cases. Specifically, without additional data, TRAIN achieves up to **8.86%** improvement in natural accuracy and **6.33%** improvement in robust accuracy.

1 Introduction

Adversarial training [1, 2, 3] has been proven to effectively defense adversarial attacks [4, 5, 6] of neural networks [7, 8]. However, models trained by adversarial training strategy have shown a significant reduction of accuracy in natural samples [9], which is usually



(a)Standard training (b)Adversarial training (c)TRAIN

Figure 1: Illustrations for representation space under different training strategies.

called *natural accuracy degradation* [40]. This problem hinders the practical application of adversarial training, as natural samples are the vast majority in reality [42].

Existing works attempt to alleviate natural accuracy degradation by data augmentation or extra data collection [46, 54], distilling classifier boundary of the standard model [10, 5, 7], instance reweighting [40], early-stopping [59], adjustments of loss functions [27], and learnable attack strategies during training [13, 16]. Nevertheless, these approaches have not fully closed the natural accuracy gap between adversarial and standard training.

Unlike previous efforts, we attempt to explain the natural accuracy degradation from a new perspective, topology. Topology refers to the neighborhood relation of data in the representation space [25]. Some adversarial training studies [24, 37] have shown the importance of topology in adversarial robustness generalization. However, they do not attenuate the negative impact on the natural samples produced by the adversarial samples, resulting in incomplete topology preservation, the natural accuracy degradation still exists.

We conjecture that adversarial training destroys the topology of natural samples in the representation space, leading to a decrease in natural accuracy. As illustrated in Fig. 1(a), a model after standard training has a well-generalizing topology of natural samples but is vulnerable to adversarial samples, which are usually far from their true class distribution in the representation space. Adversarial training pulls simultaneously the adversarial samples and their corresponding natural samples nearer [42] (Fig. 1(b)) to improve the robustness of the model while leading to the poor topological structure of the natural sample features due to the negative influence of the adversarial samples. Qualitative and quantitative analyses support the intuition that natural accuracy correlates with the topology preservation extent (see Sec. 3.2 for more details).

Inspired by the above intuition, we propose a new approach called Topology-pReserving Adversarial traINing (TRAIN) to alleviate natural accuracy degradation (Fig. 1(c)), which closes the gap between adversarial and corresponding natural samples while preserving the well-generalizing topology of the standard model. A straightforward solution is to distill the natural sample features of the standard model or the relationships based on the absolute distance between samples during adversarial training. However, it suffers from optimization difficulties due to the great gap between standard and adversarial models. So we construct the topological structure of data in the representation space based on the neighbor graph for each model. We define the edge weight of the graph as the probability that different samples are neighbors, and topology preservation is achieved by aligning the standard model’s graph and the adversarial model’s graph. Meanwhile, the optimization process of the standard model is not affected by the adversarial model, to reduce the negative impact of adversarial samples. Experiments show that benefitting from topology preservation, TRAIN improves both the natural and robust accuracy when combined with other adversarial training algorithms.

Our contributions are as follows:

- We reveal that the topology of natural samples in the representation space plays an important role in the natural accuracy of adversarial models, which provides a new perspective on mitigating natural accuracy degradation.
- We propose a *topology preservation adversarial training* method that preserves the topology structure between natural samples in the standard model representation space, which can be combined with various adversarial training methods.
- Extensive quantitative and qualitative experiments on CIFAR-10, CIFAR-100, and Tiny ImageNet datasets show the effectiveness of the proposed TRAIN (maximum 8.86% improvement for the natural accuracy and 6.33% for the robust accuracy).

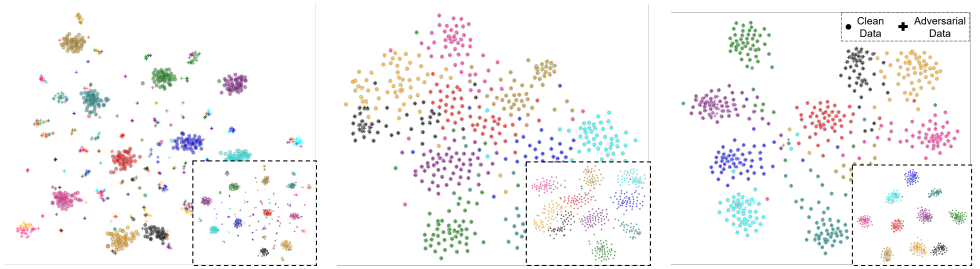
2 Related Work

2.1 Adversarial Training

Adversarial training [13, 18, 19, 28, 33, 35, 36, 38] is a prevailing method to improve the adversarial robustness of DNNs. However, it decreases the accuracy of natural samples while increasing the adversarial robustness compared with standard training. This phenomenon is called “natural accuracy degradation” or “the trade-off between robustness and accuracy”. Several works have been proposed to alleviate this problem. Zhang *et al.* [69] used early-stopping. Rebuffi *et al.* [26] tried to use more training data by data augmentation or adding extra data. Researchers [1, 5, 7] tried to distill the natural sample logits from the standard model to the adversarial model. Zhang *et al.* [40] made use of instance reweighting. Pang *et al.* [22] redefined adversarial training optimization goals. And Jia *et al.* [13] used reinforcement learning to obtain learnable attack strategies. Different from them, we mitigate this problem from the view of the topology of different data in the representation space. Some works [24, 37] show topology is crucial for adversarial robustness generalization but ignore the negative impact of adversarial examples, and still degrade in natural accuracy.

2.2 Knowledge Distillation in Adversarial Training

Knowledge distillation can transfer knowledge from a larger, cumbersome model (teacher) to a smaller, more efficient model (student), which is commonly used for model compression. Recently some algorithms have applied knowledge distillation to adversarial training. Some works [10, 44] distilled large robust models for robust model compression. Different from them, researchers [1, 5, 7] distilled the natural data logits of the standard model to enhance adversarial training on natural accuracy. [5] considered additional temperature factors during distillation. However, they did not constrain the topology of samples in the representation space, and their distillation loss updates both standard and adversarial models simultaneously. Therefore, they were still negatively affected by adversarial examples. The experimental section also includes comparative evaluations of different knowledge distillation methods.



Standard (77.39%/0.00%) TRADES (56.50%/30.93%) TRAIN (65.28%/33.97%)

Figure 2: Analytical experiments reveal the relationship between topology quality in the representation space and natural accuracy. (a), (b), and (c) show the differences in the representation space for the standard model, adversarial model (trained by TRADES with $\beta = 6.0$), and TRAIN on CIFAR-100 training (small plots), and test sets (large plots). Natural accuracy and PGD-20 accuracy are indicated in red and blue, respectively.

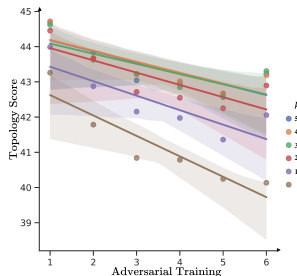


Figure 3: Quantitative analysis reveals a negative correlation between the adversarial strength and the topology score.

3 Topology’s Role in Adversarial Training

3.1 Formulation

Following vanilla AT [19], the goal of adversarial training is defined as:

$$\arg \min_{\theta} \mathbb{E}_{(x,y) \in D} \left(\max_{\delta \in S} L(x + \delta, y; \theta) \right), \quad (1)$$

where D is the data distribution for input x and its corresponding label y , θ is the model parameters. δ stands for the perturbation applied to x and is usually limited by perturbation size ϵ . $S = \{ \delta \mid \|\delta\|_p \leq \epsilon \}$ is the feasible domain for δ . $L(\cdot)$ usually is the cross-entropy loss for classification. By min-max gaming, adversarial training aims to correctly recognize all adversarial examples ($x' = x + \delta$). For descriptive purposes, we refer to models trained only on natural samples as *standard models* and those trained using adversarial training as *adversarial models* in the latter part.

3.2 Empirical Analysis

In this section, we analyze how adversarial training influences topological relationships compared with standard models. We find that the quality of the topology is positively correlated with natural accuracy, while negatively correlated with adversarial strength. Adversarial

models are trained by TRADES [68], and here we consider the weights of the adversarial loss function β as adversarial strength. Larger β represents the greater strength of adversarial training. We choose the penultimate layer representations (before logits) of the standard model and adversarial models for qualitative and quantitative experimental analysis. **See supplementary material for more details on experimental settings.**

Qualitative analysis. As shown in Fig. 2, compared with the standard model on both training the test sets, the representation visualization for adversarial models shows more robustness, but a worse topology of data resulting in lower discrimination in different classes.

Quantitative analysis. We conduct quantitative analysis by setting the $\beta = 1, 2, \dots, 6$ for TRADES as different adversarial strengths, and use k NN accuracy as the *topology score* to evaluate the quality of topology for different models, which is often used in manifold learning [24, 52] to evaluate the quality of topology in dimension reduction. The higher the score, the more reasonable topology between the samples. Specifically, we use both natural and adversarial data (generated by PGD-20) in the CIFAR-100 training set as the support set to predict the labels of natural and adversarial data in the test set. To verify the reliability of the observation conclusion, we choose $k = 5, 10, 20, 30, 40, 50$, respectively.

Fig. 3 shows the strength of adversarial training and their corresponding topology qualities for different k . A negative correlation between the strength of adversarial training and the topology quality could be observed.

Why does adversarial training destroy topological relationships? Adversarial representations are usually far away from their true class distribution, while natural samples are not. Adversarial training narrowing the adversarial representations and natural representations concurrently usually makes the representation of natural samples further away from the original distribution, and hurts the topology and discrimination of natural data representations. Zhang *et al.* [40] points out that adversarial training is equivalent to a special kind of regularization and has a strong smoothing effect, which also supports our intuition.

4 Topology-Preserving Adversarial Training

4.1 Overall Framework

To reduce the negative impact of adversarial samples, we propose a method TRAIN that focuses on preserving the topology of natural features from the standard model during adversarial training. As shown in Alg. 1, we train two models simultaneously: a standard model M with a cross-entropy loss $L_{ST}(\cdot)$ and an adversarial model M' which is updated by a specific adversarial training algorithm. For natural sample x_i , the outputs of $M(x_i)$ are the feature of the last layer f_{x_i} and logit $logit_{x_i}$. Similarly, the outputs of $M'(x'_i)$ are $f'_{x'_i}$ and $logit'_{x'_i}$ for adversarial sample x'_i and f'_{x_i} and $logit'_{x_i}$ for natural sample x_i .

The loss $L_{ST}(\cdot)$ of M is formulated as:

$$L_{ST} = L(z_{x_i}, y_i), z_{x_i} = \frac{\exp(logit_{x_i})}{\sum_{j=1}^N \exp(logit_{x_j})}, \quad (2)$$

where L is cross-entropy loss. And the overall loss $L_{AT}(\cdot)$ of M' is formulated as follows:

$$L_{AT} = L_{robust}(x') + \lambda L_{TP}(M, M'), \quad (3)$$

where $L_{robust}(\cdot)$ denotes the adversarial robustness loss, which is determined by the specific adversarial training algorithm employed. Additionally $L_{TP}(\cdot)$ serves as a regularization item

to preserve the topology of natural samples from M and updates only M' . A comprehensive discussion regarding the specifics of $L_{TP}(\cdot)$ will be discussed in the next subsection.

4.2 Topology Preservation in Adversarial Training

The topological structure is typically based on a neighborhood relation graph constructed by the similarity among samples in the representation space [21, 25, 32]. In this graph, each point is a sample in the representation space, while the edges are relationships among the samples, and the weights assigned to the edges are determined by the similarity between the samples. Consequently, the topology preservation can be precisely formulated as follows:

$$L_{TP} = \mathbb{E}_{(x,y) \in D} (F(P, Q)), \quad (4)$$

where P and Q represent the neighborhood relation graph constructed by the inter-sample similarity for M and M' , respectively. $F(\cdot)$ measures the similarity between two graphs.

Absolute relationship preservation. Directly applying cosine similarity to calculate the pairwise distances d_{ij} and d'_{ij} between samples in representation spaces of M and M' to construct the neighborhood relation graph P and Q is a straightforward way:

$$P = \{d_{ij} | 0 < i, j \leq N\}, Q = \{d'_{ij} | 0 < i, j \leq N\}, \quad (5)$$

where d_{ij} and d'_{ij} are defined as:

$$d_{ij} = 1 - \frac{f_{x_i}^T f_{x_j}}{\|f_{x_i}\|_2 \|f_{x_j}\|_2}, \tilde{d}'_{ij} = 1 - \frac{f'_{x'_i T} f'_{x'_j}}{\|f'_{x'_i}\|_2 \|f'_{x'_j}\|_2}. \quad (6)$$

However, there exists a substantial difference in the representation space between the adversarial model and the standard model, making it challenging to optimize the preservation of direct absolute relationships.

Relative relationship preservation. Considering the significant gap between standard and adversarial models, our objective is to use conditional probability distribution for modeling the relationships between samples. Specifically, we define the edge weights of the neighborhood relation graph as the probability that distinct samples are neighbors, thus ensuring topology preservation through the alignment of the probability distributions of the two graphs.

Different from manifold learning [21, 32] which uses the regular Kernel Density Estimation (KDE) for approximations of the conditional probabilities, we use the cosine similarity-based affinity metric. This choice is motivated by the excessive hyper-parameter tuning requirements and unacceptable training costs associated with KDE in adversarial training.

$$\begin{aligned} K_{cos}(f_{x_i}, f_{x_j}) &= \frac{1}{2} \left(\frac{f_{x_i}^T f_{x_j}}{\|f_{x_i}\|_2 \|f_{x_j}\|_2} + 1 \right), \\ &= \frac{1}{2} (2 - d_{ij}), \end{aligned} \quad (7)$$

where K_{cos} is cosine similarity-based affinity metric value for x_i and x_j .

Moreover, we add a special term ρ_j to better preserve the global structure of representation space. ρ_j represents the distance from the j_{th} data point to its nearest neighbor. Subtracting ρ_j ensures the local connectivity of the graph, avoiding isolated points and thus better preserves the global structure.

$$\tilde{d}_{ij} = d_{ij} - \rho_j, \tilde{d}'_{ij} = d'_{ij} - \rho'_j. \quad (8)$$

Algorithm 1 Topology-Preserving Adversarial Training

Require: the step size of perturbations ε , batch size n , learning rate α , attack algorithm optimization iteration times K , the number of training epochs T , adversarial model M' with its parameters θ' , standard model M with its parameters θ , loss weight λ and training dataset $(x, y) \in D$

Ensure: robust model M' with θ'

- 1: Randomly initialize θ, θ'
- 2: **for** $i = 1, \dots, T$ **do**
- 3: Sampling a random mini-batch $X = \{x_1, x_2, \dots, x_n\}$ and corresponding labels $Y = \{y_1, y_2, \dots, y_n\}$ from D
- 4: Generating adversarial data $X' = \{x'_1, x'_2, \dots, x'_n\}$ through attack algorithms (such as PGD-K, FGSM)
- 5: $f_X, \text{logit}_X = M(X)$
- 6: $f'_{X'}, \text{logit}'_{X'} = M'(X')$
- 7: Evaluate L_{ST} Eq. (2)
- 8: Evaluate $L_{AT} = \lambda L_{TP} + L_{\text{robust}}$ Eq. (3)
- 9: Update model parameters:
- 10: $\theta = \theta - \alpha \frac{1}{n} \sum_{i=1}^n \nabla_{\theta} L_{ST}$
- 11: $\theta' = \theta' - \alpha \frac{1}{n} \sum_{i=1}^n \nabla_{\theta'} L_{AT}$
- 12: **end for**

After normalization, we obtain the p_{ij} , which represents the conditional probability that the i_{th} natural sample is a neighbor of the j_{th} natural sample in the representation space of M .

$$p_{ij} = \frac{2 - \tilde{d}_{ij}}{\sum_{k=1, k \neq j}^N (2 - \tilde{d}_{jk})}. \quad (9)$$

Similarly, for the adversarial model M' :

$$q_{ij} = \frac{2 - \tilde{d}'_{ij}}{\sum_{k=1, k \neq j}^N (2 - \tilde{d}'_{jk})}. \quad (10)$$

So the neighborhood relation graph construction of M can be formalized as:

$$P = \left\{ p_{i|j} \mid p_{i|j} = \frac{2 - \tilde{d}_{ij}}{\sum_{k=1, k \neq j}^N (2 - \tilde{d}_{jk})}, 0 < i, j \leq N \right\}. \quad (11)$$

Similarly, the relationship graph for M' is:

$$Q = \left\{ q_{i|j} \mid q_{i|j} = \frac{2 - \tilde{d}'_{ij}}{\sum_{k=1, k \neq j}^N (2 - \tilde{d}'_{jk})}, 0 < i, j \leq N \right\}. \quad (12)$$

We use cross-entropy loss to measure the similarity of P and Q for such flexible relationships. Finally, the L_{TP} for TRAIN is formalized as:

$$\begin{aligned} L_{TP} &= CE(P, Q) \\ &= \sum_i \sum_j \left[p_{i|j} \log \left(\frac{p_{i|j}}{q_{i|j}} \right) + (1 - p_{i|j}) \log \left(\frac{1 - p_{i|j}}{1 - q_{i|j}} \right) \right]. \end{aligned} \quad (13)$$

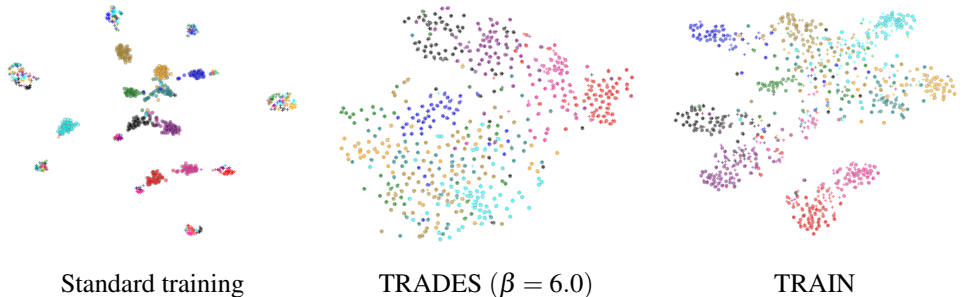


Figure 4: t-SNE visualizations of penultimate layer features on CIFAR-10. Crosses and circles are adversarial samples and natural samples, respectively. Different colors represent different classes.

5 Experiments

Experimental settings Following [10, 13, 22], we conduct extensive evaluations on popular datasets in adversarial training, including CIFAR-10, CIFAR-100 [15]. ResNet-18 is the backbone of standard models, and WideResNet-34-10 is the backbone of adversarial models. The adopted adversarial attacking method during training is PGD-10, with a perturbation size $\varepsilon = 0.031$, a step size of perturbations $\varepsilon_1 = 0.007$. For different experiment settings, we choose different λ . We set $\lambda = 5$ on CIFAR-10 dataset, and $\lambda = 20a$ on CIFAR-100 dataset, where $a = \frac{2}{1+e^{-\frac{10t}{100}-1}}$ and t is the current t -th epoch during training. Finally, all experiments were done on GeForce RTX 3090.

Our evaluation metrics are natural data accuracy (Natural Acc.) and robust accuracy (Robust Acc.). Robust accuracy is the model classification accuracy under adversarial attacks. Following previous works, we choose three representative adversarial attack methods for evaluation: PGD-20, C&W-20 [2], and Auto Attack [9]. We denote the model’s defense success rate under those attacks separately as *PGD-20 Acc.*, *C&W-20 Acc.*, and *AA Acc.*. To provide a comprehensive evaluation and comparison with other state-of-the-art adversarial training methods, we use their original hyperparameters in our settings, and include baselines: Vanilla AT [19], TRADES [38], LBGAT, MART [53], FAT [59], GAIRAT [40], AWP [66], SAT [29], LAS [13], and ECAS [16]. For TRADES, we set $\beta = 6.0$. For LBGAT, we conduct experiments based on vanilla AT and TRADES ($\beta = 6.0$). We also provide **details of experimental settings** and **experiments on Tiny ImageNet [8] in supplementary materials**.

5.1 Main Results

Quantitative results. As shown in Tables 1 and 2, TRAIN achieves a better trade-off between natural accuracy and adversarial robustness compared with the most popular adversarial training algorithms. TRADES, LBGAT, and ECAS achieve significant improvement in natural accuracy by combining with TRAIN, and the robust accuracy is also relatively improved or preserved.

Qualitative analysis. To showcase the efficacy of our algorithm in assisting the adversarial model in constructing a well-generalizing topology in the representation space, we use t-SNE to visualize samples from ten randomly selected categories in the CIFAR-100 test set and all categories of the CIFAR-10 test set for qualitative analysis. Figs. 2 and 4 show the results of CIFAR-100/10 datasets, respectively. For standard training (Figs. ?? and ??), the natural data exhibit clear clustering, while the adversarial samples appear disjointed, resulting in poor performance on robust accuracy. The TRADES approach facilitates the alignment of

Defense	Natural Acc.	Robust Acc.		
		PGD-20 Acc.	C&W-20 Acc.	AA Acc.
Vanilla AT* [10]	85.17	55.08	53.91	51.69
MART* [10]	84.17	<u>58.56</u>	54.58	51.10
FAT* [10]	87.97	49.86	48.65	47.48
GAIRAT* [10]	86.30	59.54	45.57	40.30
AWP* [10]	85.57	58.13	56.03	53.90
ECAS [10]	84.57	55.86	54.65	52.10
ECAS+TRAIN	85.26(\uparrow 0.69)	56.23(\uparrow 0.37)	54.77(\uparrow 0.12)	52.22(\uparrow 0.12)
TRADES* [10]	85.72	56.10	53.87	53.40
LAS-TRADES* [10]	85.24	57.07	55.45	54.15
TRADES + TRAIN	<u>87.07</u> (\uparrow 1.35)	58.51(\uparrow 2.41)	56.81 (\uparrow 2.94)	54.70 (\uparrow 1.30)
TRADES + LBGAT [10]	80.20	57.41	54.84	53.32
TRADES + LBGAT + TRAIN	86.69(\uparrow 6.49)	58.04(\uparrow 0.63)	<u>56.75</u> (\uparrow 1.91)	<u>54.47</u> (\uparrow 1.15)

Table 1: Results on CIFAR-10. “*” are the results directly quoted from LAS. The best and second best results are **bolded** and underlined, respectively.

Defense	Natural Acc.	Robust Acc.		
		PGD-20 Acc.	C&W-20 Acc.	AA Acc.
Vanilla AT* [10]	60.89	31.69	30.10	27.86
SAT* [10]	62.82	27.17	27.32	24.57
AWP* [10]	60.38	33.86	31.12	28.86
ECAS [10]	64.60	35.41	<u>33.39</u>	29.55
ECAS+TRAIN	65.24(\uparrow 0.64)	35.83 (\uparrow 0.42)	33.50 (\uparrow 0.11)	30.69 (\uparrow 1.14)
TRADES* [10]	58.61	28.66	27.05	25.94
LAS-TRADES* [10]	60.62	32.53	29.51	28.12
TRADES + TRAIN	67.47 (\uparrow 8.86)	34.99(\uparrow 6.33)	31.61(\uparrow 4.56)	28.95(\uparrow 3.01)
TRADES + LBGAT* [10]	60.64	34.75	30.65	29.33
TRADES + LBGAT+ TRAIN	<u>65.40</u> (\uparrow 4.76)	<u>35.46</u> (\uparrow 0.71)	32.36(\uparrow 1.71)	<u>30.17</u> (\uparrow 0.84)

Table 2: Results on CIFAR-100. “*” are the results directly quoted from LAS. The best and second best results are marked in **bold** and underline.

natural and adversarial data to enhance robust accuracy. Nonetheless, it is noteworthy that this alignment process can unintentionally disrupt the integrity of natural feature topologies, as it lacks any defensive measures to counteract this effect (refer to Figs. ?? and ?? in the paper for visual representations of this phenomenon). As shown in Figs. ?? and ??, applying the proposed TRAIN to TRADES could drive the cluster for each category to be more compact, thereby preserving the topology more effectively.

5.2 Ablation Studies

In this section, we delve into TRAIN to study its effectiveness in different relation-preserving methods. We present a comparative analysis of our proposed method with alternative approaches: a metric learning approach called MCA [57] and two absolute relationship distillation methods, namely RKD [43] and CRD [40]. MCA applies a supervised contrastive loss into adversarial training. RKD takes the absolute value of the cosine distance between samples as the relationship as discussed in Sec. 4. CRD requires that a sample’s representation in the student model be closer to its corresponding representation in the teacher model while

Methods	Natural Acc	Robust Acc		
		PGD-20 Acc	C&W-20 Acc	AA Acc
Vanilla AT [10]	60.44	28.06	27.85	24.81
MCA [57]	57.18	29.31	27.23	25.76
Vanilla AT + RKD [43]	64.00	28.32	27.92	24.92
Vanilla AT + CRD [40]	62.22	27.47	27.42	24.53
Vanilla AT + TRAIN [†]	62.10	29.43	29.66	25.78
Vanilla AT + TRAIN	66.39	29.88	29.84	25.81

Table 3: Ablation results on different relation-preserving methods.

Vanilla AT	Vanilla AT + LBGAT	Vanilla AT + TRAIN
821	848	849
TRADES	TRADES + LBGAT	TRADES + TRAIN
1,079	1,106	1,109

Table 4: Training time in second of an epoch on one RTX 3090 GPU.

being farther from the representations of other samples in the teacher model. TRAIN^f means adversarial training will influence the standard models during training. Table 3 shows the effectiveness of the relative relationship preservation TRAIN^f means adversarial training will influence the standard models during training, and it is important to reduce the negative influence of adversarial samples (comparison between TRAIN and TRAIN^f). All the ablation experiments are based on the CIFAR-100 dataset and combined with TRADES, and we provide its other training details in the supplementary material.

Time complexity. Our method is based on batch computation, and its time complexity is $O(N(mz'K)) + O(N(bz(fz' + fz) + mz))$, where mz' and mz is the number of neurons of the adversarial model (48.32 M) and standard model (11.22 M), bz is the batch size (128), fz' and fz is the feature size of the standard model (512) and adversarial model (640), and K is the number of iterations for generating adversarial examples (10). For classic adversarial training, its time complexity is $O(N(mz'K))$. Since $bz(fz' + fz) + mz \ll mz'K$, the additional time overhead of our method is negligible.

Note that, the primary time-consuming factor in adversarial training algorithms lies in the need for additional backpropagation during the generation of adversarial samples, whereas the TRAIN algorithm does not incur any extra computational cost in this regard. Table 4 shows the time statistics for training one epoch (with batch size equals 128) by different baselines. It takes an additional 28 seconds when combined with Vanilia AT and 3% (30 seconds) on TRADES for TRAIN, which is as fast as LBGAT. We also analyze **the influence of batch size, hyper-parameter λ , and model architectures in supplementary material.**

6 Conclusion

Compared with standard training, adversarial training shows significant natural accuracy degradation. Different from previous algorithms, we assume this is due to topology disruption of natural features, and confirm it by empirical experiments. Based on that, we propose Topology-pReserving Adversarial traINing (TRAIN). While improving the adversarial robustness of the model, it preserves the topology of natural samples in the representation space of the standard model. Our method has been rigorously validated through both quantitative and qualitative experiments, demonstrating its effectiveness and reliability.

7 Acknowledgments

This work is supported by the National Natural Science Foundation of China (62203425).

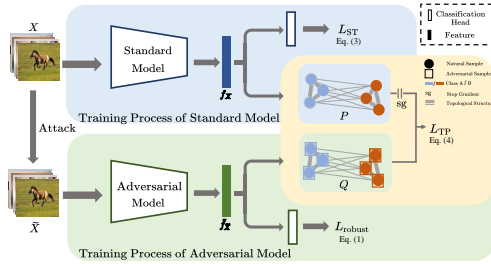


Figure 5: Overall framework of TRAIN. Specifically, we train a standard model M and an adversarial model M' . The standard model takes natural samples X as input and is optimized by cross-entropy loss. On the other hand, the adversarial model takes adversarial samples X' as input and is optimized by robust loss $L_{robust}(\cdot)$ and topology preservation loss $L_{TP}(\cdot)$. $L_{TP}(\cdot)$ constructs and aligns the neighborhood relation graph P and Q in the representation spaces of M and M' , respectively. It can preserve the topological relationships among samples to reduce the negative effects of the adversarial samples during adversarial training.

8 Supplementary Material for Topology-preserving Adversarial Training for Alleviating Natural Accuracy Degradation

8.1 Pipeline

To make it easier for the reader to understand our method, Fig. 5 shows the overall process for TRAIN combined with vanilla AT.

Discussion. LBGAT also adopts a two-model framework and transfers the prior knowledge of M to M' . Nonetheless, there exist notable distinctions between our proposed method and LBGAT, which can be summarized as follows:

1. Different perspectives. LBGAT mitigates natural accuracy degradation by focusing on the guidance of the natural classifier boundary. Different from it, our proposed TRAIN emphasizes the importance of the topology of the sample in the representation space. By combining the two perspectives, we can further enhance the model's performance, as confirmed by the experimental results.
2. Different interactions between models. In LBGAT, M and M' affect each other which still has the negative impact of the adversarial samples on the natural samples. However, when M remains independent, optimizing LBGAT becomes challenging due to the inherent differences between the two models. In TRAIN, M unidirectionally influences M' and as an anchor to preserve the original topology of natural samples in the representation space to avoid the negative influence of the adversarial samples on the natural samples. This design choice effectively mitigates the adverse effects of adversarial samples on natural samples.

These differentiating factors highlight the unique contributions of our proposed TRAIN method in addressing the natural accuracy degradation during adversarial training. By considering the topological aspects of samples to avoid the negative impact of adversarial samples, TRAIN offers a novel and effective approach for enhancing model robustness and performance.

8.2 The Flexibility of TRAIN

Different from other methods, TRAIN mitigates natural accuracy degradation by adopting a novel topological perspective. Moreover, TRAIN could be applied to other adversarial training methods, such as vanilla AT [19], TRADES [68], and LBGAT [2], in a plug-and-play way. To validate the effectiveness of our proposed enhancements, we conduct comprehensive validation experiments on these strong baselines. We have introduced the robust loss of vanilla AT in our paper. TRADES [68] improves classification performance by introducing a regularization term, which penalizes the discrepancy between the logits for adversarial examples and their corresponding natural images. Its optimization objective is defined as:

$$\arg \min_{\theta} \mathbb{E}_{(x,y) \in D} \left(L(x, y; \theta) + \beta \max_{\delta \in S} L(x + \delta, x; \theta) \right), \quad (14)$$

where β is a hyper-parameter and its value means the strength of regularization for robustness. TRADES has proven highly effective and remains a strong baseline for adversarial training to this day. Here we will elucidate the specifics of our approach when integrated with another strong baseline LBGAT.

LBGAT leverages the model logits obtained from a standard model to guide the learning process of an adversarial model. It is usually combined with vanilla AT and TRADES. The total loss L_{AT} of adversarial model M' combined with LBGAT and vanilla AT is:

$$\begin{aligned} L_{AT} = & L(z'_{x_i}, y_i) + \gamma \| \text{logit}'_{x'_i} - \text{logit}_{x_i} \|_2 \\ & + \lambda \sum_i \sum_j \left[p_{i|j} \log \left(\frac{p_{i|j}}{q_{i|j}} \right) + (1 - p_{i|j}) \log \left(\frac{1 - p_{i|j}}{1 - q_{i|j}} \right) \right], \end{aligned} \quad (15)$$

and the total loss of adversarial model L_{AT} combined with LBGAT and TRADES is:

$$\begin{aligned} L_{AT} = & L(z'_{x_i}, y_i) + \beta KL(z'_{x_i} || z'_{x'_i}) + \gamma \| \text{logit}'_{x'_i} - \text{logit}_{x_i} \|_2 \\ & + \lambda \sum_i \sum_j \left[p_{i|j} \log \left(\frac{p_{i|j}}{q_{i|j}} \right) + (1 - p_{i|j}) \log \left(\frac{1 - p_{i|j}}{1 - q_{i|j}} \right) \right], \end{aligned} \quad (16)$$

$$z'_{x_i} = \frac{\exp(\text{logit}'_{x_i})}{\sum_{j=1}^N \exp(\text{logit}'_{x_j})}, z'_{x'_i} = \frac{\exp(\text{logit}'_{x'_i})}{\sum_{j=1}^N \exp(\text{logit}'_{x'_j})},$$

where KL is Kullback–Leibler divergence, which is commonly used to concretely implement the robust regularization of TRADES. γ is the hyper-parameter of LBGAT, and β is the hyper-parameter of TRADES.

8.3 Experimental Settings

Datasets. Following [2, 13, 22], we conduct extensive evaluations on popular datasets, including CIFAR-10, CIFAR-100 [13] and Tiny ImageNet [8] dataset to validate the effectiveness of our algorithm. The CIFAR-10 and CIFAR-100 datasets consist of a total of 60,000 color images with dimensions of 32×32 pixels. Among these 50,000 images are designated for training and the remaining 10,000 images are reserved for testing. Furthermore, CIFAR-10 has 10 categories while CIFAR-100 has 100 categories. Furthermore, the Tiny ImageNet dataset includes 120,000 color images with dimensions of 64×64 pixels in 200 categories,

with each category containing 500 training images, 50 validation images, and 50 testing images. This dataset offers a larger image size and a broader range of categories, enabling a more challenging evaluation of our algorithm’s performance.

Baselines. We choose three strong baselines to demonstrate the effectiveness of our method: Vanilla AT [19], TRADES [58], and LBGAT. For TRADES, we set $\beta = 6.0$. For LBGAT, we conduct experiments based on vanilla AT and TRADES ($\beta = 6.0$). We also add ALP [24] as a baseline in the Tiny ImageNet dataset. In addition, we combine TRAIN with them to demonstrate the superiority of our approach. To provide a comprehensive evaluation and comparison with other state-of-the-art adversarial training methods, we include additional baseline: MART [33], FAT [39], GAIRAT [40], AWP [36], SAT [29], LAS [13], and ECAS [16].

Evaluation metrics. To evaluate the generalization of the model on natural and adversarial samples, our evaluation metrics are natural data accuracy (Natural Acc.) and robust accuracy (Robust Acc.). Robust accuracy is the model classification accuracy under adversarial attacks. As specified in the respective publications, we choose three representative adversarial attack methods for evaluation: PGD-20, C&W-20 [9], and Auto Attack [9]. We denote the model’s defense success rate under those attacks separately as *PGD-20 Acc.*, *C&W-20 Acc.*, and *AA Acc.*. Similar to manifold learning, we make *k*NN test accuracy as a topology score due to *k*NN relying solely on the relationships among samples to classify. We utilize training sets as support sets (natural samples and adversarial samples generated by PGD-20) and methods [21, 32]. In Fig. 3 we set *k* as 5, 10, 20, 30, 40, 50, and we observe that the choice of *k* does not affect the relative ranking of the topological relationships among samples in different representation spaces. So in Tables 5 and 6, we set *k* as 30.

Data pre-process. Similar to LBGAT [9], for CIFAR-10/100 datasets, the input size of each image is 32×32 , and the training data is normalized to $[0, 1]$ after standard data augmentation: random crops of 4 pixels padding size and random horizontal flip, and the test set is normalized to $[0, 1]$ without any extra augmentation; For the training set of Tiny ImageNet, we resize the image from 64×64 to 32×32 , and the data augmentation is random crops with 4 pixels of padding; finally, we normalize pixel values to $[0, 1]$, and for the test set, we resize the image to 32×32 and normalize pixel values to $[0, 1]$. Others are the same as CIFAR datasets.

Training details. For Tables 1 and 2, we follow state-of-the-art adversarial training method LAS [13]. ϵ is $8/255$, and The initial learning rate is set to 0.1 with a total of 110 epochs for training and reduced to 0.1x at the 100-th and 105-th epochs. Weight decay is 5×10^{-4} , and random seed is 1. ResNet-18 is the backbone of standard models, and WideResNet-34-10 is the backbone of adversarial models. The adopted adversarial attacking method during training is PGD-10, with a perturbation size $\epsilon = 0.031$, a step size of perturbations $\epsilon_1 = 0.007$. For different experiment settings, we choose different λ . We set $\lambda = 5$ on CIFAR-10 dataset, and $\lambda = 20a$ on CIFAR-100 dataset, where $a = \frac{2}{1+e^{-\frac{10r}{100}-1}}$ and *t* is the current *t*-th epoch during training. Finally, all experiments were done on GeForce RTX 3090.

8.4 Sensitivity of different learning rate

Experimental settings. For Table 5, Table 6, qualitative experiments, and all ablation experiments, we keep the same super-parameter configuration as LBGAT [9]. The initial learning rate is set to 0.1 with a total of 100 epochs for training and reduced to 0.1x at the 75-th and

Defense	Natural Acc.	Robust Acc.			Topology Score	
		PGD-20 Acc.	C&W-20 Acc.	AA Acc.	Natural	Robust
Standard Training	94.46	0.00	0.00	0.00	94.94	-
Vanilla AT [C]	86.69	53.45	53.72	48.95	86.51	53.94
Vanilla AT + TRAIN	88.85 (\uparrow 2.16)	55.64 (\uparrow 2.19)	56.18 (\uparrow 2.46)	50.89 (\uparrow 1.94)	89.11 (\uparrow 2.60)	56.55 (\uparrow 2.61)
Vanilla AT + LBGAT [D]	86.55	54.34	53.35	47.27	86.64	54.26
Vanilla AT + LBGAT + TRAIN	89.42 (\uparrow 2.87)	56.21 (\uparrow 1.87)	57.48 (\uparrow 4.13)	51.77 (\uparrow 4.50)	89.25 (\uparrow 2.61)	56.59 (\uparrow 2.33)
TRADES* [E]	84.42	56.59	54.91	51.91	85.58	56.73
TRADES + TRAIN	87.30 (\uparrow 2.88)	58.20 (\uparrow 1.61)	56.31 (\uparrow 1.40)	53.09 (\uparrow 1.18)	90.01 (\uparrow 4.43)	58.86 (\uparrow 2.13)
TRADES + LBGAT* [F]	81.98	57.78	55.53	53.14	84.57	57.79
TRADES + LBGAT + TRAIN	87.62 (\uparrow 5.64)	57.73(\downarrow 0.05)	58.08 (\uparrow 2.55)	53.64 (\uparrow 0.50)	89.50 (\uparrow 5.00)	57.98(\uparrow 0.19)

Table 5: Results on CIFAR-10. When added to the existing baseline under most settings, our method achieves both natural accuracy and robust accuracy improvements, particularly in terms of C&W-20 Acc. “*” are the results directly quoted from LBGAT.

90-th epochs. The optimization algorithm is SGD, with a momentum of 0.9 and weight decay of 2×10^{-4} . Moreover, all our experimental results are reproducible with a random seed of 1.

Our method exhibits superior performance when applied with the new hyperparameters. According to Tables 5 and 6, TRAIN can effectively increase both natural and robust accuracy, and contribute to the topology preservation of both natural and adversarial samples.

In Table 5, TRAIN gets an improvement by 2.16% compared to vanilla AT baseline on natural data. It surpasses vanilla AT on PGD-20, C&W, and AA accuracy by 2.19%, 2.46%, and 1.94% respectively, indicating its high robustness. Our method also has improvements on LBGAT by 4.50% to 1.87% in all aspects. For another common baseline, TRADES, TRAIN also gets competitive results on both natural and adversarial data. Note that natural accuracy decreases when applying LBGAT to TRADES, so it also brings a large enhancement when combined with our method. For the topology score which is measured by k NN accuracy, TRAIN could boost the performance by a large margin. Since k NN classification is based only on inter-sample relationships, such results prove that TRAIN could mitigate topology disruptions of both natural and adversarial samples from adversarial training.

The overall results on CIFAR-100 are similar to CIFAR-10. As shown in Table 6, TRAIN performs better than vanilla AT and LBGAT and gets a further improvement when deployed with LBGAT simultaneously. For TRADES, our method surpasses it by a large margin (8.78%) on natural data and improves the robust accuracy by 3.04%. Adding LBGAT to TRAIN causes a decrease in natural accuracy but achieves the best accuracy in PGD-20 and C&W-20. The above results show that the proposed TRAIN could be applied to popular adversarial training pipelines for achieving SOTA performance on both natural accuracy and robust accuracy. Despite a slight decrease in individual robust metrics, we have achieved a better balance between natural accuracy and adversarial robustness overall. For the topology score, we can find that combining the baseline with TRAIN can further enhance the quality of topology for both natural and adversarial samples in the representation space.

8.5 Quantitative results on Tiny ImageNet.

To demonstrate the effectiveness of our approach on a highly demanding dataset, we performed rigorous experiments on the Tiny Imagenet dataset. The results, as depicted in Table 7, clearly demonstrate that the combination of our algorithm with TRADES and LBGAT techniques leads to substantial improvements in both natural accuracy and adversarial robustness. When combined with Trades, our approach achieves a 2.61% improvement in natural accuracy and

Defense	Natural Acc.		Robust Acc.		Topology Score	
	PGD-20 Acc.	C&W-20 Acc.	AA Acc.	Natural	Robust	
Standard Training	77.39	0.00	0.00	0.00	77.07	-
Vanilla AT [C]	60.44	28.06	27.85	24.81	57.17	31.32
Vanilla AT + TRAIN	66.39 ($\uparrow 5.95$)	29.88 ($\uparrow 1.82$)	29.84 ($\uparrow 1.99$)	25.81 ($\uparrow 1.00$)	64.70 ($\uparrow 7.53$)	32.84 ($\uparrow 1.52$)
Vanilla AT + LBGAT [D]	61.01	30.10	28.09	25.63	61.28	30.47
Vanilla AT + LBGAT + TRAIN	68.20 ($\uparrow 7.19$)	29.83 ($\downarrow 0.27$)	30.84 ($\uparrow 2.75$)	25.88 ($\uparrow 0.25$)	66.08 ($\uparrow 4.80$)	32.48 ($\uparrow 2.01$)
TRADES* [E]	56.50	30.93	28.43	26.87	52.57	32.17
TRADES + TRAIN	65.28 ($\uparrow 8.78$)	33.97 ($\uparrow 3.04$)	30.86 ($\uparrow 2.43$)	28.25 ($\uparrow 1.38$)	65.78 ($\uparrow 13.21$)	34.53 ($\uparrow 2.36$)
TRADES + LBGAT* [D]	60.43	35.50	31.50	29.34	61.06	37.52
TRADES + LBGAT + TRAIN	62.62 ($\uparrow 2.19$)	36.27 ($\uparrow 0.77$)	31.72 ($\uparrow 0.22$)	29.19($\downarrow 0.15$)	64.84 ($\uparrow 3.78$)	38.25 ($\uparrow 0.73$)

Table 6: Results on CIFAR-100. Similar to Table 5, our method can improve the natural accuracy (up to 8.78%), robust accuracy (up to 3.04%), and topology score (up to 13.21%) of baselines. “*” are the results directly quoted from LBGAT.

Defense	Clean Acc.	PGD-20 Acc.
Vanilla AT* [C]	30.65	6.81
Vanilla AT + LBGAT* [D]	36.50	14.00
ALP* [E]	30.51	8.01
LBGAT + ALP* [D]	33.67	14.55
TRADES ($\beta = 6.0$)* [E]	38.51	13.48
TRADES ($\beta = 6.0$) + LBGAT* [D]	39.26	16.42
TRADES ($\beta = 6.0$) + Ours	41.12($\uparrow 2.61$)	16.18($\uparrow 2.70$)
TRADES ($\beta = 6.0$) + LBGAT + Ours	41.53 ($\uparrow 2.27$)	17.09 ($\uparrow 0.67$)

Table 7: Quantitative experiment on Tiny ImageNet. “*” are the results directly quoted from LBGAT.

a 2.70% improvement in robust accuracy. When combined with TRADES+LBGAT, our method achieves a 2.27% improvement in natural accuracy and a 0.67% improvement in robust accuracy.

8.6 More Ablation Studies

In this section, we delve into TRAIN to study its effectiveness in batch size, hyper-parameter λ , and model architectures. We also analyze the time complexity and training time of our method. All the ablation experiments are based on the CIFAR-100 dataset and combined with TRADES. All ablation experimental settings (**including ablation on different relationship preservation methods in our paper**) are the same as Tables 5 and 6.

Backbone of M'	Training Strategy	Backbone of M	Clean Acc.	Robust Acc.		
				PGD-20 Acc.	C&W-20 Acc.	AA Acc.
None	Standard Training	ResNet-18	77.39	0	0	0
WideResNet34-10	TRADES + Ours	ResNet-18	62.62	36.27	31.72	29.19
None	Standard Training	WideResNet34-10	78.11	0	0	0
WideResNet34-10	TRADES + Ours	WideResNet34-10	63.09	35.54	30.41	28.76

Table 8: The ablation experiment about different backbones of the standard model.

Impact of batch size. As shown in Table 9, we tried 128, 256, 384 samples per batch for relation calculating. Among them, a batch size of 256 achieves the best results, but the difference among different batch sizes is not large. Overall our method is not sensitive to different batch sizes.

To ensure fair comparisons with other methods, we chose a batch size of 128 for our other experiments.

Batch Size	Natural Acc.	Robust Acc.		
		PGD-20 Acc.	C&W-20 Acc.	AA Acc.
128	66.39	29.88	29.84	25.81
256	66.55	31.08	30.72	26.07
384	66.26	30.60	30.16	25.41

Table 9: The ablation experiment about different batch sizes.

	0	5a	10a	20a	50a
Natural Acc.	57.99	61.52	63.21	65.28	66.40
PGD-20 Acc.	31.53	32.31	33.47	33.90	33.62
L_{TP}	0.66	0.35	0.32	0.27	0.24

Table 10: Sensitivity analysis of hyper-parameter λ .

Sensitivity analysis of hyper-parameter λ . As Table 10 shows, with the increase of λ in Eq. (3), natural accuracy always gets higher; L_{TP} (calculated from the test set) gets lower; while the PGD-20 accuracy rises at first and then remains stable. It is reasonable because a large λ forces the topology of clean samples to be highly close to that of standard models. Finally, we set λ as 20a according to the PGD-20 accuracy following [19].

Impact of the different standard models. As depicted in Table 8, our approach exhibits robustness to variations in the backbones of standard models. Specifically, we observe that ResNet18 achieves a comparable trade-off between natural accuracy and adversarial robustness to WideresNet34-10 on the CIFAR-100 datasets while incurring lower training costs.

Table 11 shows the results of using different standard training strategies. To expedite the training process, a pre-trained standard model can be used in TRAIN (vanilla AT+TRAIN*). However, training the standard model and adversarial model jointly achieves superior results. This is attributed to the fact that the representation spaces of the two joint models are closer, facilitating optimization procedures.

Methods	Clean Acc	Robust Acc		
		PGD-20 Acc	C&W-20 Acc	AA Acc
Vanilla AT	35.10	18.89	16.19	14.63
Vanilla AT+ TRAIN	38.58	20.25	17.64	15.39
TRADES	38.39	17.90	14.36	13.38
TRADES +TRAIN	43.64	18.52	14.86	13.51

Table 12: Experiments using MobileNetv3 on CIFAR100.

Impact of different backbones of M' . We conduct experiments on MobileNetv3, and the results reinforce the effectiveness of our approach across different backbones. As shown in Table 12, our method can further improve the baseline, especially in natural accuracy. We achieve a maximum improvement of 5.25% in natural accuracy and a maximum improvement of 1.45% in robust accuracy.

We can also find that the experimental results on MobileNet v3 are inferior compared to WideResNet34-10, both in terms of robustness and natural sample accuracy. This observation can be attributed to the positive correlation between the effectiveness of adversarial training algorithms and model capacity [3], and to reduce inference speed, MobileNet v3 has a significantly smaller model capacity compared to WideResNet34-10.

Methods	Clean Acc	Robust Acc		
		PGD-20 Acc	C&W-20 Acc	AA Acc
Vanilla AT	60.44	28.06	27.85	24.81
Vanilla AT + TRAIN*	65.15	28.00	27.90	24.91
Vanilla AT + TRAIN	66.39	29.88	29.84	25.81

Table 11: Ablation experiment about different standard models on CIFAR-100. TRAIN* means using a well-trained standard model, and TRAIN means training two models jointly.

References

- [1] Elahe Arani, Fahad Sarfraz, and Bahram Zonooz. Adversarial concurrent training: Optimizing robustness and accuracy trade-off of deep neural networks. *arXiv preprint arXiv:2008.07015*, 2020.
- [2] Anish Athalye, Nicholas Carlini, and David Wagner. Obfuscated gradients give a false sense of security: Circumventing defenses to adversarial examples. In *International conference on machine learning*, pages 274–283. PMLR, 2018.
- [3] Tao Bai, Jinqi Luo, Jun Zhao, Bihan Wen, and Qian Wang. Recent advances in adversarial training for adversarial robustness. *arXiv preprint arXiv:2102.01356*, 2021.
- [4] Nicholas Carlini and David Wagner. Towards evaluating the robustness of neural networks. In *2017 IEEE Symposium on Security and Privacy (SP)*, pages 39–57. IEEE, 2017.
- [5] Erh-Chung Chen and Che-Rung Lee. Ltd: Low temperature distillation for robust adversarial training. *arXiv preprint arXiv:2111.02331*, 2021.
- [6] Francesco Croce and Matthias Hein. Reliable evaluation of adversarial robustness with an ensemble of diverse parameter-free attacks. In *International conference on machine learning*, pages 2206–2216. PMLR, 2020.
- [7] Jiequan Cui, Shu Liu, Liwei Wang, and Jiaya Jia. Learnable boundary guided adversarial training. In *Proceedings of the IEEE/CVF International Conference on Computer Vision*, pages 15721–15730, 2021.
- [8] Jia Deng, Wei Dong, Richard Socher, Li-Jia Li, Kai Li, and Li Fei-Fei. Imagenet: A large-scale hierarchical image database. In *2009 IEEE conference on computer vision and pattern recognition*, pages 248–255. Ieee, 2009.
- [9] Haoran Gao, Hua Zhang, Xin Zhang, Wenmin Li, Jiahui Wang, and Fei Gao. Enhanced covertness class discriminative universal adversarial perturbations. *Neural Networks*, 165:516–526, 2023. ISSN 0893-6080. doi: <https://doi.org/10.1016/j.neunet.2023.06.006>. URL <https://www.sciencedirect.com/science/article/pii/S0893608023003076>.
- [10] Micah Goldblum, Liam Fowl, Soheil Feizi, and Tom Goldstein. Adversarially robust distillation. In *Proceedings of the AAAI Conference on Artificial Intelligence*, volume 34, pages 3996–4003, 2020.

- [11] Lirong He, Qingzhong Ai, Xincheng Yang, Yazhou Ren, Qifan Wang, and Zenglin Xu. Boosting adversarial robustness via self-paced adversarial training. *Neural Networks*, 167:706–714, 2023. ISSN 0893-6080. doi: <https://doi.org/10.1016/j.neunet.2023.08.063>. URL <https://www.sciencedirect.com/science/article/pii/S0893608023004938>.
- [12] Pei Huang, Yuting Yang, Minghao Liu, Fuqi Jia, Feifei Ma, and Jian Zhang. ϵ -weakened robustness of deep neural networks. In *Proceedings of the 31st ACM SIGSOFT International Symposium on Software Testing and Analysis, ISSTA 2022*, page 126–138, New York, NY, USA, 2022. Association for Computing Machinery. ISBN 9781450393799. doi: 10.1145/3533767.3534373. URL <https://doi.org/10.1145/3533767.3534373>.
- [13] Xiaojun Jia, Yong Zhang, Baoyuan Wu, Ke Ma, Jue Wang, and Xiaochun Cao. Las-at: Adversarial training with learnable attack strategy. In *Proceedings of the IEEE/CVF Conference on Computer Vision and Pattern Recognition*, pages 13398–13408, 2022.
- [14] Harini Kannan, Alexey Kurakin, and Ian Goodfellow. Adversarial logit pairing. *arXiv preprint arXiv:1803.06373*, 2018.
- [15] Alex Krizhevsky, Geoffrey Hinton, et al. Learning multiple layers of features from tiny images. 2009.
- [16] Hui Kuurila-Zhang, Haoyu Chen, and Guoying Zhao. Adaptive adversarial norm space for efficient adversarial training. In *34th British Machine Vision Conference Proceedings*. BMVA Press, 2023.
- [17] Huanhuan Li, Wenbo Yu, and He Huang. Strengthening transferability of adversarial examples by adaptive inertia and amplitude spectrum dropout. *Neural Networks*, 165:925–937, 2023. ISSN 0893-6080. doi: <https://doi.org/10.1016/j.neunet.2023.06.031>. URL <https://www.sciencedirect.com/science/article/pii/S089360802300343X>.
- [18] Tao Li, Yingwen Wu, Sizhe Chen, Kun Fang, and Xiaolin Huang. Subspace adversarial training. *arXiv preprint arXiv:2111.12229*, 2021.
- [19] Aleksander Madry, Aleksandar Makelov, Ludwig Schmidt, Dimitris Tsipras, and Adrian Vladu. Towards deep learning models resistant to adversarial attacks. *arXiv preprint arXiv:1706.06083*, 2017.
- [20] Chengzhi Mao, Ziyuan Zhong, Junfeng Yang, Carl Vondrick, and Baishakhi Ray. Metric learning for adversarial robustness. *Advances in Neural Information Processing Systems*, 32, 2019.
- [21] Leland McInnes, John Healy, and James Melville. UMAP: Uniform Manifold Approximation and Projection for Dimension Reduction. *arXiv preprint arXiv:1802.03426*, 2018.
- [22] Tianyu Pang, Min Lin, Xiao Yang, Jun Zhu, and Shuicheng Yan. Robustness and accuracy could be reconcilable by (proper) definition. 2022.

- [23] Wonpyo Park, Dongju Kim, Yan Lu, and Minsu Cho. Relational knowledge distillation. In *Proceedings of the IEEE/CVF Conference on Computer Vision and Pattern Recognition*, pages 3967–3976, 2019.
- [24] Zhuang Qian, Shufei Zhang, Kaizhu Huang, Qiufeng Wang, Rui Zhang, and Xinpeng Yi. Improving model robustness with latent distribution locally and globally. *arXiv preprint arXiv:2107.04401*, 2021.
- [25] Juan Ramon Rabunal, Julian Dorado, and Alejandro Pazos Sierra. *Encyclopedia of artificial intelligence*. IGI Global, 2009.
- [26] Sylvestre-Alvise Rebuffi, Sven Gowal, Dan Andrei Calian, Florian Stimberg, Olivia Wiles, and Timothy A Mann. Data augmentation can improve robustness. *Advances in Neural Information Processing Systems*, 34:29935–29948, 2021.
- [27] Lukas Schott, Jonas Rauber, Matthias Bethge, and Wieland Brendel. Towards the first adversarially robust neural network model on mnist. *arXiv preprint arXiv:1805.09190*, 2018.
- [28] Naman Deep Singh, Francesco Croce, and Matthias Hein. Revisiting adversarial training for imagenet: Architectures, training and generalization across threat models. *Advances in Neural Information Processing Systems*, 36, 2023.
- [29] Chawin Sitawarin, Supriyo Chakraborty, and David Wagner. Sat: Improving adversarial training via curriculum-based loss smoothing. In *Proceedings of the 14th ACM Workshop on Artificial Intelligence and Security*, pages 25–36, 2021.
- [30] Yonglong Tian, Dilip Krishnan, and Phillip Isola. Contrastive representation distillation. In *International Conference on Learning Representations*, 2019.
- [31] Florian Tramer, Nicholas Carlini, Wieland Brendel, and Aleksander Madry. On adaptive attacks to adversarial example defenses. *Advances in Neural Information Processing Systems*, 33:1633–1645, 2020.
- [32] Laurens Van der Maaten and Geoffrey Hinton. Visualizing data using t-SNE. *Journal of machine learning research*, 9(11), 2008.
- [33] Yisen Wang, Difan Zou, Jinfeng Yi, James Bailey, Xingjun Ma, and Quanquan Gu. Improving adversarial robustness requires revisiting misclassified examples. In *International Conference on Learning Representations*, 2019.
- [34] Zekai Wang, Tianyu Pang, Chao Du, Min Lin, Weiwei Liu, and Shuicheng Yan. Better diffusion models further improve adversarial training. In Andreas Krause, Emma Brunskill, Kyunghyun Cho, Barbara Engelhardt, Sivan Sabato, and Jonathan Scarlett, editors, *Proceedings of the 40th International Conference on Machine Learning*, volume 202 of *Proceedings of Machine Learning Research*, pages 36246–36263. PMLR, 23–29 Jul 2023. URL <https://proceedings.mlr.press/v202/wang23ad.html>.
- [35] Eric Wong, Leslie Rice, and J Zico Kolter. Fast is better than free: Revisiting adversarial training. *arXiv preprint arXiv:2001.03994*, 2020.

- [36] Dongxian Wu, Shu-Tao Xia, and Yisen Wang. Adversarial weight perturbation helps robust generalization. *Advances in Neural Information Processing Systems*, 33:2958–2969, 2020.
- [37] Shuo Yang, Zeyu Feng, Pei Du, Bo Du, and Chang Xu. Structure-aware stabilization of adversarial robustness with massive contrastive adversaries. In *2021 IEEE International Conference on Data Mining (ICDM)*, pages 807–816. IEEE, 2021.
- [38] Hongyang Zhang, Yaodong Yu, Jiantao Jiao, Eric Xing, Laurent El Ghaoui, and Michael Jordan. Theoretically principled trade-off between robustness and accuracy. In *International conference on machine learning*, pages 7472–7482. PMLR, 2019.
- [39] Jingfeng Zhang, Xilie Xu, Bo Han, Gang Niu, Lizhen Cui, Masashi Sugiyama, and Mohan Kankanhalli. Attacks which do not kill training make adversarial learning stronger. In *International conference on machine learning*, pages 11278–11287. PMLR, 2020.
- [40] Jingfeng Zhang, Jianing Zhu, Gang Niu, Bo Han, Masashi Sugiyama, and Mohan S Kankanhalli. Geometry-aware instance-reweighted adversarial training. In *ICLR*, 2021.
- [41] Bojia Zi, Shihao Zhao, Xingjun Ma, and Yu-Gang Jiang. Revisiting adversarial robustness distillation: Robust soft labels make student better. In *Proceedings of the IEEE/CVF International Conference on Computer Vision*, pages 16443–16452, 2021.